CHAPTER 15

A NUMERICAL MODEL FOR REFRACTION COMPUTATION OF IRREGULAR WAVES DUE TO TIME-VARYING CURRENTS AND WATER DEPTH

Masataka Yamaguchi[1] and Yoshio Hatada[2]

ABSTRACT

This paper presents two models for current-depth refraction of directional spectra due to time-varying currents and water depth, in which a piecewise ray method and a full ray method are used for numerical computations respectively. The results computed by the piecewise ray model in the cases of time-varying one-dimensional and two-dimensional currents are in reasonable agreement with those by the full ray model, which gives the almost exact solution in the case of linear current and water depth variations, except for a slight difference during the phase of strong opposing currents. The computations indicate that time-dependency of currents gives rise to a phase difference between wave height and current variations, and reduction in the amplification effect of directional spectrum due to opposing currents in comparison with steady current case.

1. INTRODUCTION

It is empirically known that waves are greatly amplified by the presence of strong opposing currents and that waves affected by tidal currents vary regularly with a pseudo-period of tidal currents (Vincent, 1979). As an example, Fig. 1 describes the time variation of significant waves observed at Naruto Strait which is located between Shikoku Island and Awaji Island. Naruto Strait is very famous for strong tidal currents and tide-induced large scale vortices. The investigation of such a phenomenon which might be caused by wave-current interac-

---

1 Prof., Dept. of Ocean Eng., Ehime Univ., Bunkyocho 3, Matsuyama 790, Ehime Pref., Japan
2 Research Assistant, Dept. of Ocean Eng., Ehime Univ., Bunkyocho 3, Matsuyama 790, Ehime Pref., Japan

tion, and the establishment of the evaluation method are of great importance for mitigation of coastal hazard, design of maritime structures, ship operation and so on.

Fig. 2 is a classification of the existing current-depth refraction models for irregular waves. The previous models assume time-independent fields for currents and water depth. Recently, Yamaguchi et al.(1988) and Tolman(1988) proposed numerical models applicable to the refraction computation of irregular waves with time-varying currents and water depth. The former model is a generalization of the time-independent model by Mathiesen (1984) and

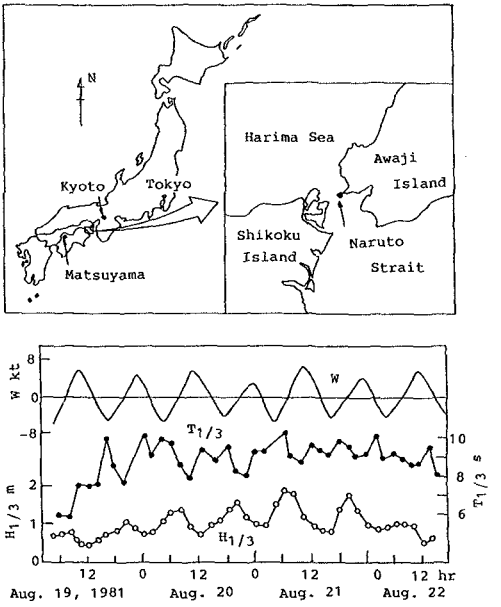

Fig. 1 Naruto Strait, and observed tidal currents and significant waves.

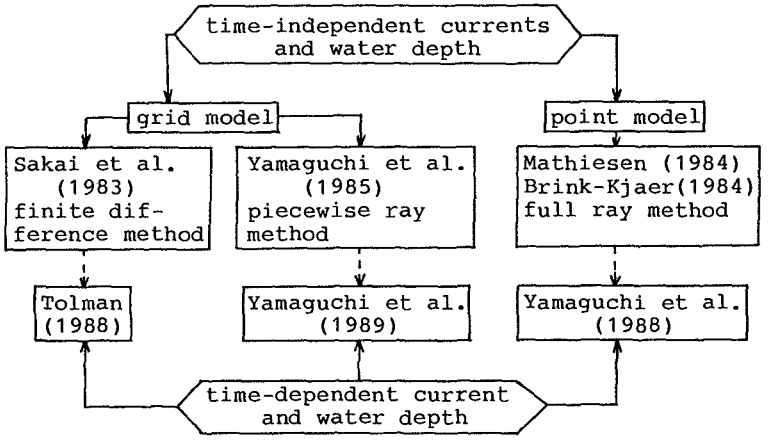

Fig. 2 A classification of current-depth refraction models for irregular waves.

Brink-Kjaer(1984) using a full ray method hereafter referred to as point model or full ray model, and the latter model is an extension of the time-independent model by Sakai et al.(1983) based on a finite difference method to a time-dependent model. Yamaguchi et al.(1989) also developed another numerical model for the refraction computation of directional spectra due to time-varying currents and water depth, which is a generalization of the authors' model(1985) based on a piecewise ray method hereafter referred to as grid model or piecewise ray model.

The aim of this study is to present two models for the time-dependent current-depth refraction of irregular waves developed by the authors and some examples of the numerical computation based on both models. First, the computation methods used in the models are explained in detail. Next, the models are applied to the computation of wave refraction caused by time-varying one-dimensional and two-dimensional model currents on a uniformly sloping beach. The accuracy of the piecewise ray model is investigated in comparison with the results based on the full ray model. The effect of time-dependency of currents and water depth on wave transformation is also examined from the comparison with the results for steady current case.

2. MODEL DESCRIPTIONS

(1) Basic Equations

The basic equations used in the model are the conservation equation for wave action density spectrum N(k) defined by the ratio of wave number spectrum E(k) to intrinsic angular frequency σ_m ,

$$\frac{\partial N(k)}{\partial t}+(C_g\cos\theta+U)\frac{\partial N(k)}{\partial x}+(C_g\sin\theta+V)\frac{\partial N(k)}{\partial y}+\frac{dk_x}{dt}\frac{\partial N(k)}{\partial k_x}+\frac{dk_y}{dt}\frac{\partial N(k)}{\partial k_y}=0 \tag{1}$$

a set of equations for wave number vector components k_x and k_y,

$$\frac{\partial k_x}{\partial t}+(C_g\cos\theta+U)\frac{\partial k_x}{\partial x}+(C_g\sin\theta+V)\frac{\partial k_x}{\partial y}=-\frac{gk^2\,\mathrm{sech}^2 kh}{2\sigma_m}\frac{\partial h}{\partial x}-k_x\frac{\partial U}{\partial x}-k_y\frac{\partial V}{\partial x} \tag{2}$$

$$\frac{\partial k_y}{\partial t}+(C_g\cos\theta+U)\frac{\partial k_y}{\partial x}+(C_g\sin\theta+V)\frac{\partial k_y}{\partial y}=-\frac{gk^2\,\mathrm{sech}^2 kh}{2\sigma_m}\frac{\partial h}{\partial y}-k_x\frac{\partial U}{\partial y}-k_y\frac{\partial V}{\partial y} \tag{3}$$

the Doppler relation,

$$\sigma=\sigma_m+k_xU+k_yV\ , \qquad \sigma_m=\sqrt{gk\tanh kh} \tag{4}$$

and the equation of absolute angular frequency σ

$$\frac{\partial\sigma}{\partial t}+(C_g\cos\theta+U)\frac{\partial\sigma}{\partial x}+(C_g\sin\theta+V)\frac{\partial\sigma}{\partial y}$$

$$=\frac{gk^2\,\mathrm{sech}^2 kh}{2\sigma_m}\frac{\partial h}{\partial t}+k_x\frac{\partial U}{\partial t}+k_y\frac{\partial V}{\partial t} \tag{5}$$

where C_g is the group velocity of a component wave, θ the wave direction, k the wave number, $k_x=k\cos\theta$, $k_y=k\sin\theta$, h the water depth, g the acceleration of gravity and (U,V) are the current components. Eq. (2) to Eq. (5) are not mutually independent, as is clear from their derivation. We choose the three equations, Eq. (2) to Eq. (4) for their relative simplicity of computation.

Eq. (1) means that even in the case of time-varying currents and water depth, the action spectrum for each wave component is conserved along the wave ray defined by

$$\frac{dx}{dt}=C_g\cos\theta+U, \quad \frac{dy}{dt}=C_g\sin\theta+V \tag{6}$$

where the wave number components are computed from

$$\frac{dk_x}{dt}=-\frac{gk^2\,\mathrm{sech}^2 kh}{2\sigma_m}\frac{\partial h}{\partial x}-k_x\frac{\partial U}{\partial x}-k_y\frac{\partial V}{\partial x} \tag{7}$$

$$\frac{dk_y}{dt}=-\frac{gk^2\,\mathrm{sech}^2 kh}{2\sigma_m}\frac{\partial h}{\partial y}-k_x\frac{\partial U}{\partial y}-k_y\frac{\partial V}{\partial y} \tag{8}$$

Thus, the conservation of the action spectrum $\psi(f,\theta)$ in frequency-direction space (f,θ) is written as

$$\begin{aligned}\psi(f,\theta)&=|(C_{g1}+U_1\cos\theta_1+V_1\sin\theta_1)/2\pi k_1\sigma_{m1}|\,E(f_1,\theta_1)\\&=|(C_{g2}+U_2\cos\theta_2+V_2\sin\theta_2)/2\pi k_2\sigma_{m2}|\,E(f_2,\theta_2)\\&=|(C_g+U\cos\theta+V\sin\theta)/2\pi k\sigma_m|\,E(f,\theta)\\&=\Phi(f,\theta)E(f,\theta)=\text{const.}\end{aligned} \tag{9}$$

where f is the absolute frequency, $\Phi(f,\theta)$ the amplification factor due to current-depth refraction, $E(f,\theta)$ is the directional spectrum, and subscripts '1' and '2' are used for denoting different time as well as different place. This is the basic relationship used to compute current-depth refraction of directional spectrum.

Wave statistics are obtained by the numerical integration over wave direction and frequency using

$$E(f)=\int_0^{\pi}E(f,\theta)d\theta, \quad \varepsilon=\int_0^{\infty}E(f)df\ , \quad H_{1/3}=4\sqrt{\varepsilon},$$

$$T_{1/3}=1.22\sqrt{\varepsilon\Big/\int_0^{\infty}f^2E(f)df}\ , \quad \bar{\theta}=\tan^{-1}\left\{\frac{\int_0^{\infty}\int_0^{\pi}E(f,\theta)\sin\theta d\theta df}{\int_0^{\infty}\int_0^{\pi}E(f,\theta)\cos\theta d\theta df}\right\} \tag{10}$$

where E(f) is the frequency spectrum, ε the total wave energy, $H_{1/3}$ the significant wave height, $T_{1/3}$ the significant wave period and $\bar{\theta}$ the mean wave direction.

The input directional spectrum is given as

$$E_0(f,\theta)=E_0(f)\cdot D_0(f,\theta) \tag{11}$$

where D(f, θ) is the angular spreading function and subscript '0' indicates the offshore boundary. The frequency spectrum and angular spreading function rely on the Bretscneider-Mitsuyasu type spectrum and the Mitsuyasu type function respectively. They are expressed as

$$E_0(f)=0.257\,H_{1/3}^{(0)2}T_{1/3}^{(0)}(T_{1/3}^{(0)}f)^{-5}\exp\left[-1.03(T_{1/3}^{(0)}f)^{-4}\right] \tag{12}$$

$$D_0(f,\theta)=\frac{1}{\pi}2^{2S-1}\frac{\Gamma^2(S+1)}{\Gamma(2S+1)}\cos^{2S}\frac{(\theta-\theta_w)}{2},\quad S=\begin{cases}S_{max}(f/f_{op})^5 & ;f<f_{op}\\ S_{max}(f/f_{op})^{-2.5} & ;f\geqq f_{op}\end{cases} \tag{13}$$

where S and S_{max} are the energy concentration factor and its maximum value, θ_w the principal wave direction, Γ the gamma function, $f_{op}(=1/1.05T_{1/3})$ the peak frequency, and superscript '(0)' denotes the offshore boundary as well as the above-mentioned subscript '0'.

(2) Numerical Methods

a. Piecewise ray model: The basic idea in the numerical computation is to assume that the action spectrum of a component wave of interest at an inner point (x,y) at t-Δt-time, $\phi(f_r^{t-\Delta t}, \theta_s^{t-\Delta t}; x, y, t-\Delta t)$ becomes the one at a grid point (i,j) at t-time, $\phi(f_p, \theta_q; i, j, t)$ after propagation along a ray over time increment Δt, where subscripts ('r', 'p') and ('s', 'q') denote the frequency and direction at different positions and times respectively, and the directional spectrum at a grid point (i,j) at t-time, $E(f_p, \theta_q; i, j, t)$ can be evaluated using the action spectrum $\phi(f_p, \theta_q; i, j, t)$ and the characteristics of a component wave, water depth and current components at the same grid point and time, $(C_g^t, k^t, \sigma_m^t, h^t, U^t, V^t)$. Time-variability and inhomogeneity of current and water depth fields induce changes of not only wave direction but also absolute frequency of a component wave with its propagation.

A piecewise ray method is used to obtain the horizontal distribution of wave characteristics. The method consists of two steps. The first step is to trace all wave ray components from the grid points backward by one time step Δt, as shown in Fig. 3. Each wave ray is followed by solving the equations of wave number vector components, Eqs. (2) and (3) with the Runge-Kutta method under initial values of wave number components at a starting grid point. The initial values are estimated from iterative numerical solution of the Doppler relation, Eq. (5) under the given conditions of absolute frequency,

wave direction, water depth and current components. It should be noted that there exist sets of cut-off direction and frequency where propagation of directional spectrum is blocked. In the ray computation, input wave direction and current direction are reversed, and current components and water depth at the ray tip are interpolated not only in space but also in time owing to their time-dependency.

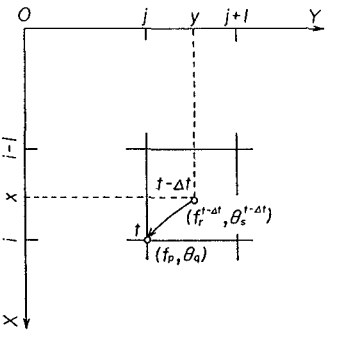

Fig. 3 Backward piecewise ray tracing.

The second step is to interpolate the action spectrum at the ray tip for the wave direction and absolute frequency shifted due to refraction. First, the Lagrange interpolation formula with third order accuracy is applied to the action spectra at the grid points surrounding the ray tip in order to estimate the action spectra for six sets of the prescribed input wave directions and absolute frequencies, namely two input wave directions(θ_n , θ_{n+1}) putting the refracted wave direction at the ray tip $\theta_s^{t-\Delta t}$ between them, and three input frequencies (f_{m-1}, f_m, f_{m+1}) putting the shifted absolute frequency at the ray tip $f_r^{t-\Delta t}$ among them. The formula is given as

$$\psi_{i+r,j+s}=\sum_{I=i-1}^{i+2}\sum_{J=j-1}^{j+2}\left(\prod_{k\neq I}\frac{x-x_k}{x_I-x_k}\right)\left(\prod_{l\neq J}\frac{y-y_l}{y_J-y_l}\right)\psi_{IJ}$$

$$r=(x-[x])/\Delta x\ ,\ s=(y-[y])/\Delta y \qquad (14)$$

Second, the action spectrum at the ray tip for the refracted wave direction and the input frequency is obtained by a linear interpolation over wave direction of the action spectra for the input wave directions estimated every input frequency as

$$\psi(f_k,\ \theta_s^{t-\Delta t};\ x,\ y,\ t-\Delta t)=\psi(f_k,\ \theta_n;\ x,\ y,\ t-\Delta t)+\{\psi(f_k,\ \theta_{n+1};\ x,\ y,\ t-\Delta t)-\psi(f_k,\ \theta_n;\ x,\ y,\ t-\Delta t)\}\cdot(\theta_s^{t-\Delta t}-\theta_n)/(\theta_{n+1}-\theta_n) \qquad (15)$$

where k (=m-1, m, m+1) means the index of input frequency. Third, the action spectrum at the ray tip for refracted wave direction and frequency is estimated by use of parabolic interpolation of the log-transformed action spectra with respect to frequency as

$$\log\psi(f_r^{t-\Delta t},\ \theta_s^{t-\Delta t};\ x,\ y,\ t-\Delta t)=a(\log f_r^{t-\Delta t})^2+b(\log f_r^{t-\Delta t})+c \qquad (16)$$

where a, b and c are the coefficients in a parabola curve determined from three sets of $\{\ f_k,\ \psi(f_k,\ \theta_s^{t-\Delta t};\ x,\ y,\ t-\Delta t)\ \}$, $k=m-1,\ m,\ m+1$. This procedure is required because the frequency of each wave component changes due to time-variation of currents and water depth.

b. Full ray model: The basic idea used in the model is the same as the one in the piecewise ray model. The computation in the full ray model consists of two steps.

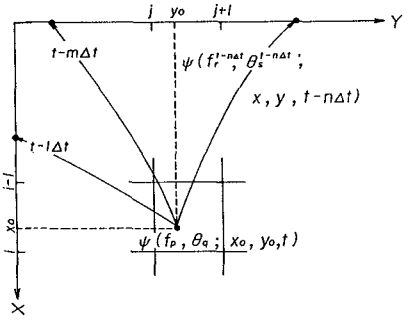

Fig. 4 Backward full ray tracing.

The first step is to trace the wave ray of a component wave backward from a selected computation point to the grid boundary by the numerical integration of Eqs. (2) and (3) with the Runge-Kutta method, as illustrated in Fig. 4. In the ray tracing, currents and water depth at the ray tip are interpolated from those at the grid points, taking into account their space and time dependency.

The second step is to estimate the action spectrum at grid boundary for frequency and direction shifted due to refraction at an arrival time of the ray, using input data for directional spectra. It should be emphasized that the arrival time of each ray is different. By iterating these procedures every direction and frequency, directional spectra at a certain time at the prescribed position can be computed.

The full ray model can give the almost exact solution in a simple case of linear currents and uniformly sloping bottom, because errors associated with interpolation are negligibly small, but it is less advantageous for the evaluation of horizontal distribution of wave characteristics when compared to the piecewise ray model, as the computation is conducted separately and independently at each position.

3. COMPUTATIONAL RESULTS AND CONSIDERATIONS

(1) One-dimensional current case

Fig. 5 shows the computation region with a grid spacing of $\Delta x=4$ km and a spatial distribution of sinusoidally-varying unsteady one-dimensional linear currents with period of $\widetilde{T}=12$ hours on a uniformly sloping beach of $i=1/1000$. The currents are given by

$$U=0, \quad V=\begin{cases} -0.2(j-4)\sin|(k-1)\pi/6| & ; j\geqq 4 \\ 0 & ; j<4 \end{cases} \tag{17}$$

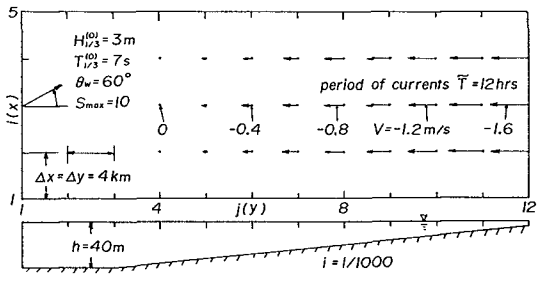

Fig. 5 Computation region and current distribution.

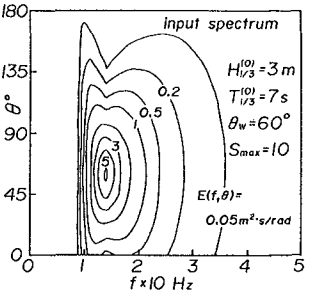

Fig. 6 Input directional spectra.

where k is the index denoting the time of the input currents given every 1 hour. The input wave conditions at the offshore boundary are also indicated in the figure. The 30 unevenly-spaced frequency data ranging from 0.09 to 0.571 Hz and the 37 evenly-spaced direction data from 0 to 180° are used with a time increment of 5 min. We focus our discussion on the wave characteristics at the grid point where water depth is 8 m deep and maximum current velocity is 1.4 m/s. Fig. 6 is the contour plot of input directional spectra.

Fig. 7 is the comparison between the time variations of wave height computed by both the full ray model and the piecewise ray model. The figure contains time variations of a current component V and wave height at the offshore boundary $\tilde{H}_{1/3}^{(0)}$. This wave height is different from the input wave height given in the directional spectral model, Eqs. (11) to (13), defined on the entire circle(θ =0 - 360°), because the computation is conducted on the half circle(θ =0 - 180°). Both models are in close agreement except for a slight difference during the phase of opposing currents. The figure also shows that time-dependency of currents brings about a phase shift between the time variations of wave height and currents, and reduction in the amplification effect of wave height due to opposing currents in comparison with the steady current case.

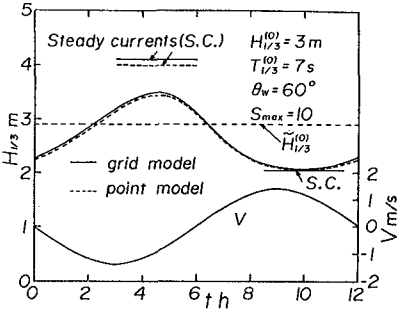

Fig. 7 Time-variation of wave heights with unsteady one-dimennal currents.

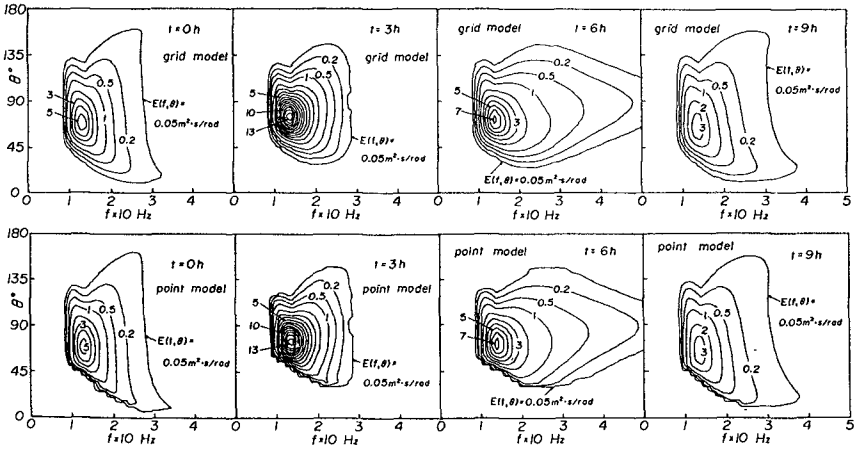

Fig. 8 Time variations of directional spectra with unsteady one-dimensional currents.

Fig. 8 describes the variations every 3 hours of the directional spectra at the before-mentioned point computed by both models. Shrinking and expanding of the distribution of directional spectra associated with temporal variation of currents are observed in the figure. Comparison between the results with the piecewise ray model and those with the full ray model suggests that both models give similar distributions of directional spectra at each time, although the piecewise ray model predicts smoother distribution in the vicinity of cut-off direction and frequency by use of interpolation formulas in the computation of action spectrum.

(2) Two-dimensional current case

Current-depth refraction of directional spectra induced by sinusoidally-varying unsteady two-dimensional model currents with period of $\tilde{T}$=6 hours shown in Fig. 9 was computed on a uniformly sloping beach of i=1/250 divided into 17x10 with a grid spacing of 1 km. This current pattern is a modeling of tidal currents flowing in and out of a river mouth. The 18 unevenly-spaced frequency data from 0.09 to 0.351 Hz and the 37

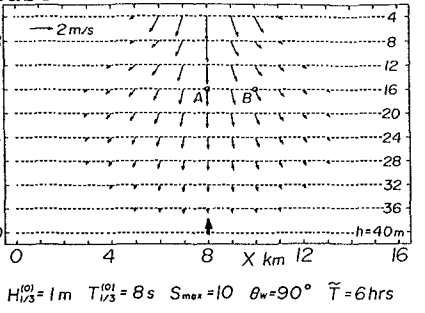

Fig. 9 An example of two dimensional current patterns given in the computation.

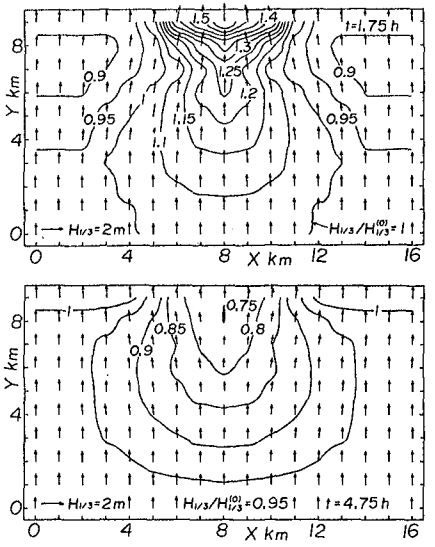

Fig. 10 Spatial distribution of wave heights and directions with unsteady two-dimensional currents.

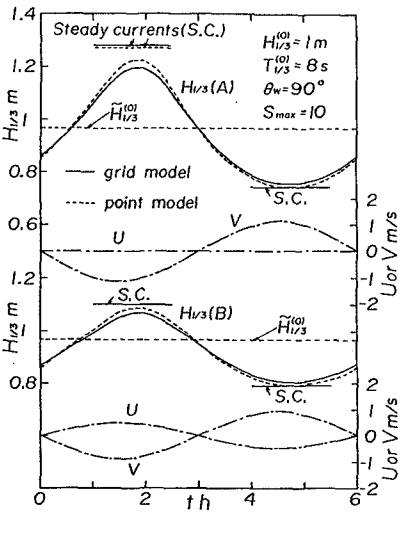

Fig. 11 Time variation of wave heights with unsteady two-dimensional currents.

evenly-spaced direction data are used with a time increment of 1.5 min. Input wave conditions are given in the figure. The computation making use of the symmetry of the solution was carried out to save computer processing time. We concentrate our concern on the change of wave characteristics at the points A and B except for wave height distribution.

Fig. 10 illustrates the horizontal distribution of wave height and wave direction at the phase of almost maximum opposing currents and the one at the phase of almost maximum following currents respectively, which are obtained by use of the piecewise ray model. At the phase of opposing currents, waves tend to converge toward the river mouth and wave height increases rapidly. But the amplification ratio is not so large as that in the case of steady opposing currents, as seen in the one-dimensional currents case. On the other hand, at the phase of following currents, waves tend to refract so as to be away from the river mouth and wave height reduces slowly compared to the opposing current case.

Fig. 11 shows the time variations of currents and wave height at the points A and B computed with both models.

The wave height variation follows the current variation behind about 1 hour. Due to energy leakage introduced through the repeated interpolation of action spectra, the piecewise ray model gives slightly smaller variation of wave height, when compared to the full ray model.

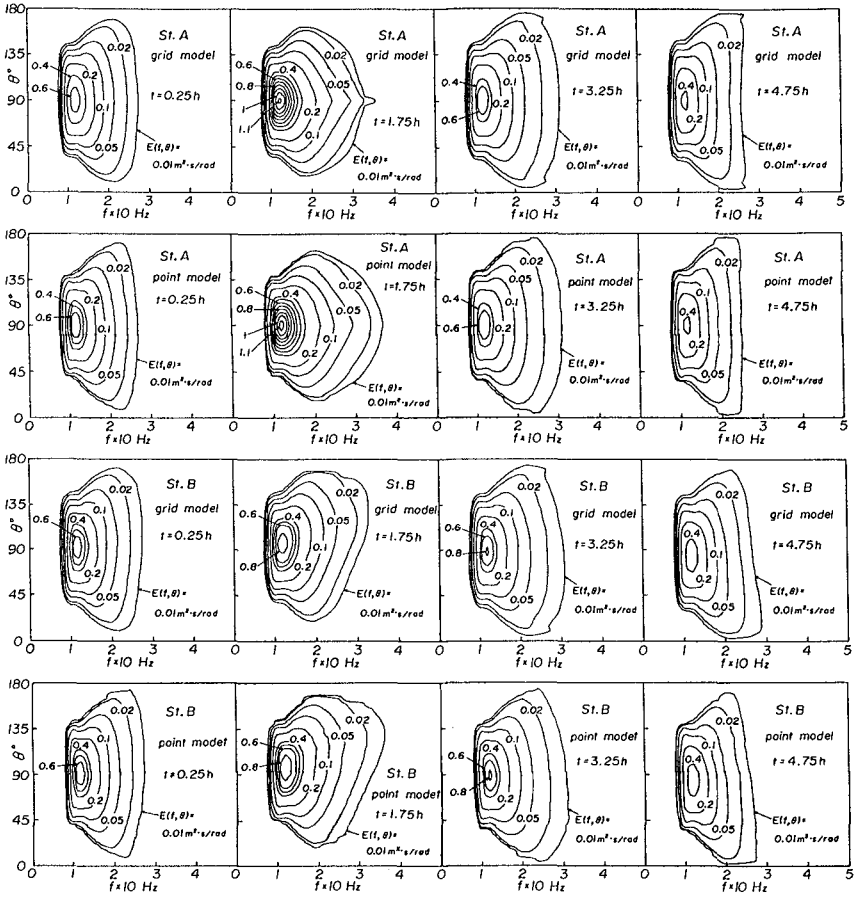

Fig. 12 Time variation of directional spectra with unsteady two-dimensional currents.

The time variations of directional spectra at the points A and B computed with both models are illustrated in Fig. 12. Both models produce close agreement in general patterns of directional spectra, but the distribution with the piecewise ray model are slightly smoother than those with the full ray model as well as the

case of one-dimensional currents. Convergence and divergence of the directional spectral distribution are alternately repeated with time-variation in direction and velocity of currents.

The directional spectra at the point A has a symmetrical distribution with respect to $\theta = 90^\circ$ axis. Whereas at the point B of some distance from the center line of the region, component waves with directions of 90 to 180° receive stronger effect of currents than those with directions of 0 to 90° because of the current direction, and the resulting directional spectra at the phase of maximum opposing currents and those at the phase of maximum following currents have asymmetrical distribution relative to input wave direction. But, at the phase of zero currents, directional spectra have quasi-symmetrical distribution and the effect of currents is not clear.

4. CONCLUSIONS

The results obtained in this study are summarized as follows;

1) Two models for current-depth refraction of directional spectra due to time-varying currents and water depth are established,in which a piecewise ray method and a full ray method are used in numerical computation for propagation of directional spectra respectively.
2) The results computed with the piecewise ray model in the cases of time-varying one-dimensional and two-dimensional currents are in relatively close agreement with those by the full ray model except for a slight difference associated with the repeated interpolation of action spectra.
3) Time-dependency of currents gives rise to a time lag between wave height and current variations, and reduction in the amplification effect of directional spectrum due to opposing currents in comparison with steady current case.

5. ACKNOWLEDGEMENTS

Thanks are due to Mr. M. Ohfuku, Technical Officer, Department of Ocean Engineering, Ehime University, for his sincere help during the study. A part of this study was accomplished with the support of the Science Research Fund (No. 01550408) of the Ministry of Education, for which the authors express their appreciation.

REFERENCES

Brink-Kjaer (1984): Depth-current refraction of wave spectra, Sympo. on Description and Modelling of Directional Seas, C-7-1-12.

Mathiesen, M. (1984): Current-depth refraction of directional spectra, Sympo. on Description and Modelling of Directional Seas, C-6-1-8.

Sakai, T. et al. (1983): Irregular wave refraction due to current, Jour. of Hydraul. Eng., ASCE, Vol. 109, pp. 1203-1215.

Tolman, H. L. (1988): Propagation of wind waves on tide, Proc. of 21st ICCE, Vol. 1, pp. 512-523.

Vincent, C. E. (1979): The interaction of wind-generated sea waves with tidal currents, Jour. of Phys. Oceanogr., Vol. 9, pp. 748-755.

Yamaguchi, M. et al. (1985): Numerical models for wave transformation due to current-depth refraction, Proc. of JSCE, Vol. 357/II-3, pp. 187-195(in Japanese).

Yamaguchi, M. et al. (1988): A numerical model for refraction computation due to time-varying currents, water depth and incident waves, Natural Disas. Science, Vol. 7-1, pp. 1-9(in Japanese).

Yamaguchi, M. et al. (1989): A numerical model for refraction computation of irregular waves due to time-varying currents and water depth, Proc. of JSCE, Vol. 405/II-11, pp. 225-234(in Japanese).